PHYSICAL REVIEW LETTERS **122,** 253603 (2019)

Cavity Dark Mode of Distant Coupled Atom-Cavity Systems

Donald H. White,[1] Shinya Kato,[1,2] Nikolett Német,[3,4] Scott Parkins,[3,4] and Takao Aoki[1,*]
[1]*Department of Applied Physics, Waseda University, 3-4-1 Okubo, Shinjuku, Tokyo 169-8555, Japan*
[2]*JST PRESTO, 4-1-8 Honcho, Kawaguchi, Saitama 332-0012, Japan*
[3]*Dodd-Walls Centre for Photonic and Quantum Technologies, New Zealand*
[4]*Department of Physics, University of Auckland, Auckland 1010, New Zealand*

(Received 28 March 2019; published 28 June 2019)

We report on a combined experimental and theoretical investigation into the normal modes of an all-fiber coupled cavity-quantum-electrodynamics system. The interaction between atomic ensembles and photons in the same cavities, and that between the photons in these cavities and the photons in the fiber connecting these cavities, generates five nondegenerate normal modes. We demonstrate our ability to excite each normal mode individually. We study particularly the "cavity dark mode," in which the two cavities coupled directly to the atoms do not exhibit photonic excitation. Through the observation of this mode, we demonstrate remote excitation and nonlocal saturation of atoms.

DOI: 10.1103/PhysRevLett.122.253603

A future quantum internet depends on the connection and entanglement of many distant qubits [1,2]. These qubits form the nodes of the network, and communication between nodes is carried via channels that transmit quantum information. When coupling between the nodes is bidirectional [3], instead of unidirectional [4,5], the system oscillates as a collective whole, and the oscillations can be projected onto a set of orthogonal normal modes in which energy is continuously exchanged between oscillators. This normal mode behavior defines the structural basis of the system dynamics, underlying the higher-level dynamical effects leading to, e.g., operation of quantum gates [6] and the physical implementation of systems of strongly interacting photons [7–9].

All-fiber atom-cavity quantum electrodynamics (QED) systems, in which atoms are coupled to the cavity field via evanescent coupling through a tapered optical nanofiber region, are an especially attractive prospect for quantum networking due to the ease of connecting many nodes together in any arbitrary network configuration with minimal loss. A cavity QED system is typically formed by coupling the atoms to an in-fiber cavity formed by either two fiber Bragg gratings (FBGs) [10–15] or else a ring cavity coupled via a fiber beam splitter [16–18]. This Letter is focused on "coupled-cavities quantum electrodynamics," concerning the interaction of atoms coupled via cavity fields. Specifically, we focus on the properties of the normal modes of two atomic ensembles coupled via three optical cavities.

A dark mode is a class of normal modes in which one or more oscillators does not exhibit excitation due to destructive interference. An example of such a mode is a dark atomic state, which is prevented from absorbing a photon due to coupling induced by control fields [19]. In addition to the widely used application of electromagnetically induced transparency [20], the dark mode of a coupled system has, for example, been used to suppress mechanical dissipation in an optomechanical resonator [21]. We recently demonstrated the "fiber dark mode" of a coupled-cavity QED system, where distant atoms interact with delocalized photons [22]. We show in this Letter that another type of dark normal mode exists in this system, in which the photonic excitations at the atom locations are dark, such that the atoms are not locally exposed to light fields. This "cavity dark mode" is robust and does not depend on cavity symmetry. With the absence of local photons, we demonstrate nonlocal excitation and saturation of atoms.

The experiment comprises an elementary all-fiber quantum network, similar to our previous setup [22], in which two nanofiber cavity QED systems are connected by an intermediate link fiber cavity, as illustrated in Fig. 1(a) (in this Letter, the two cavities directly coupled to atoms are named "cavities," while the linking fiber cavity is referred to as the "fiber"). Optical cavities are formed within the single-mode optical fiber between FBG mirrors, and atoms are coupled to the cavities via tapered fiber regions of diameter 400 nm. We experimentally excite and detect the five normal modes of this network of five coupled oscillators (three optical cavities and two ^{133}Cs atomic ensembles), which are illustrated in Fig. 1(b). These modes are strongly coupled, such that they are spectrally separate and able to be individually excited [22]. In this Letter we focus specifically on the observation of the cavity dark mode [mode (v) in Fig. 1(b)], and the corresponding observations of remote atom excitation and nonlocal atomic saturation. The two cavities are oscillation nodes of this mode, meaning that the two distant atomic ensembles communicate only via the remote link fiber. We emphasize that this is

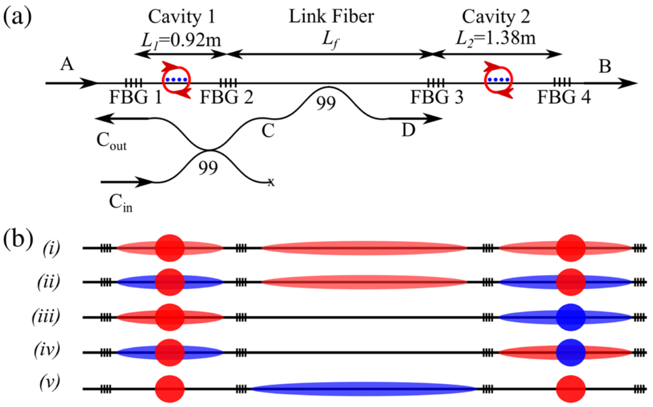

FIG. 1. (a) Schematic of the setup. Three optical cavities, comprising four fiber Bragg grating mirrors, are connected in series. Optical nanofiber regions are fabricated within the two end cavities, enabling coupling to ensembles of atoms through the evanescent field. The system may be probed from either the cavity end (A) or from the central fiber beam splitter (C), while the excitation is simultaneously detected at ports B and C. (b) Schematic of normal modes of the system. Ellipses indicate cavity excitations, and circles indicate atom excitations. Red and blue are π out of phase. Five normal modes are present: (i),(ii) are symmetric bright modes, (iii),(iv) are fiber dark modes, and (v) is the cavity dark mode.

a truly macroscopic network: the cavities are each of order 1 m long. This observation of all normal modes of a macroscopically large quantum network, observed simultaneously at two points of the network, lays the foundation for extension to larger networks of multiple atom-cavity systems for quantum information processing purposes.

Let us first consider the system with one atom for each cavity, whose Hamiltonian ($\hbar = 1$) is given by

$$H = \omega_c(a_1^\dagger a_1 + a_2^\dagger a_2 + b^\dagger b) + \sum_{i=1,2} v_i(a_i^\dagger b + b^\dagger a_i) + \omega_a(\sigma_1^+\sigma_1^- + \sigma_2^+\sigma_2^-) + \sum_{i=1,2} g_i(a_i^\dagger \sigma_i^- + \sigma_i^+ a_i), \qquad (1)$$

where we assume that the cavity and fiber modes (a_1, a_2, b) are degenerate with frequency ω_c. The coupling rates of cavities 1 and 2 with the fiber are given by

$$v_{1,2} = \frac{c}{2}\sqrt{\frac{T_{2,3}}{L_f L_{1,2}}}, \qquad (2)$$

where c is the speed of light in the fiber and T_i, L_i, and L_f are the transmittance of the mirror i, length of the cavity i, and length of the connecting fiber, respectively. The atoms are coupled to their respective cavity modes with strengths g_1 and g_2. The eigenstates of the above Hamiltonian are given by superpositions of certain combinations of the atom excitations, and the photons in the two cavities and the fiber. The eigenstates for the first excited states are given by the superpositions of the base states $|A_1\rangle = |e, g, 0, 0, 0\rangle$, $|A_2\rangle = |g, e, 0, 0, 0\rangle$, $|C_1\rangle = |g, g, 1, 0, 0\rangle$, $|C_2\rangle = |g, g, 0, 1, 0\rangle$, $|C_\mathrm{f}\rangle = |g, g, 0, 0, 1\rangle$, where $|i_1, i_2, n_1, n_2, n_\mathrm{f}\rangle$ denotes the state of the total system with atom 1 and 2 in the states i_1 and i_2, and cavity 1, 2, and the fiber in the Fock states of photon numbers n_1, n_2, and n_f. Specifically, for the simple case of $\omega_c = \omega_a \equiv \omega_0$, $g_1 = g_2 \equiv g$, and $v_1 = v_2 \equiv v$, the eigenstates and eigenenergies are given by

$$\begin{aligned}
&\text{(i)} && |\mathrm{BS1}\rangle \propto g|A_1\rangle + g|A_2\rangle + \zeta|C_1\rangle && \\
& && \quad + \zeta|C_2\rangle + 2v|F\rangle, && \omega_0 + \zeta, \\
&\text{(ii)} && |\mathrm{BS2}\rangle \propto g|A_1\rangle + g|A_2\rangle - \zeta|C_1\rangle && \\
& && \quad - \zeta|C_2\rangle + 2v|F\rangle, && \omega_0 - \zeta, \\
&\text{(iii)} && |\mathrm{FD1}\rangle \propto |A_1\rangle - |A_2\rangle + |C_1\rangle - |C_2\rangle, && \omega_0 + g, \\
&\text{(iv)} && |\mathrm{FD2}\rangle \propto |A_1\rangle - |A_2\rangle - |C_1\rangle + |C_2\rangle, && \omega_0 - g, \\
&\text{(v)} && |\mathrm{CD}\rangle \propto v|A_1\rangle + v|A_2\rangle - g|F\rangle, && \omega_0,
\end{aligned}$$

where $\zeta = \sqrt{g^2 + 2v^2}$ is the symmetric mode resonance shift. The modes (i)–(v) are illustrated in Fig. 1(b). The two states of (i) $|\mathrm{BS1}\rangle$ and (ii) $|\mathrm{BS2}\rangle$ are "bright states" and have photon excitations in the two cavities and the fiber. In contrast, the other three are "dark states," where photon excitations are absent either from the link fiber or from the two end cavities. Two states—the fiber dark states of (iii) $|\mathrm{FD1}\rangle$ and (iv) $|\mathrm{FD2}\rangle$—do not exhibit excitation in the central link fiber. Of particular interest is the cavity dark state (v) $|\mathrm{CD}\rangle$, which has no photon excitation in the two cavities in which atoms are placed. In other words, it is the state of atoms dressed with the remote photons of the link fiber. We emphasize that this state exists only when atoms are coherently coupled to both cavities. For the general case with $g_1 \neq g_2$ and $v_1 \neq v_2$, the states of (iii) $|\mathrm{FD1}\rangle$ and (iv) $|\mathrm{FD2}\rangle$ are no longer pure fiber dark states, although for the parameters discussed in this work the fiber contribution is negligibly small (see Supplemental Material [23]). The state (v) $|\mathrm{CD}\rangle$ remains a pure cavity dark state independent of cavity symmetry.

These eigenstates (i)–(v) correspond to the normal modes of the system dynamics in the weak-driving limit [23], as illustrated in Fig. 1(b). For a system with ensembles of atoms in the cavities, the linear optical response in the weak-driving limit is identical to the single-atom model, in which the single-atom coupling strengths g_i are replaced by the effective coupling strengths $g_{i,\mathrm{eff}} = g_i\sqrt{N_{i,\mathrm{eff}}}$, where $N_{i,\mathrm{eff}}$ is the effective number of atoms in cavity i [22].

The setup is similar to that of our previous work [22], where we observed four of the five normal modes: the two symmetric modes (i) and (ii), and the two fiber dark modes (iii) and (iv). In our previous work, we directly excited cavity 1 and detected the response of cavity 2. Both of these cavities are nodes of the cavity dark mode (v), meaning that we could not detect this mode in the original work. In this experiment, we introduce a fiber beam splitter into the link fiber to study this unique mode of oscillation. Specifically, the setup shown in Fig. 1(a) is designed to allow the system to be driven and detected at either the end of the cavity array (ports *A* and *B*), or through a fiber beam splitter at the central link fiber (port *C*). The response of one network node at port *B* is simultaneously observed with the response of the link fiber at port *C*. This enables experimental probing of all normal modes, and provides simultaneous access to cavity oscillation nodes and antinodes. The weak 1% outcoupling of the beam splitter ensures that the normal modes are not excessively broadened by loss.

An experimental run consists of three main steps. First, laser-cooled Cs atoms in the $6^2S_{1/2}F = 4$ state are loaded from a magneto-optical trap into a compensated evanescent-field far-off-resonant dipole trap (FORT) [24–27]. An optical lattice of 937 nm light and a repulsive 688 nm beam are present in the nanofiber region to form the series of trap sites. Second, spectroscopy is performed on the atom-cavity system by sweeping a probe laser, input either at port *A* or *C*, from −30 to +30 MHz with respect to the atomic and bare-cavity resonances. Third, the atoms are optically pumped into the dark $F = 3$ state, and spectroscopy is performed on the effectively empty-cavity condition with input at port *A*. Single-photon counting modules (SPCMs) detect the response at ports *B* and *C* for both frequency sweeps.

We first show the results of driving the input port *A* in Fig. 2, similar to our previous work [22], but this time measuring the two output ports *B* and *C* simultaneously. The $A \rightarrow B$ transmissions in Figs. 2(a) and 2(c) reproduce the observation of the fiber dark modes and the bright modes in Ref. [22]. Furthermore, the naming of the fiber dark modes is supported by the suppression of the corresponding peaks in the $A \rightarrow C$ transmissions in Figs. 2(b) and 2(d). Only the bright modes have excitation at both the end cavity and the link fiber, and therefore can be driven and detected in this $A \rightarrow C$ configuration. The data agree with the theoretical curve of the steady-state solution for the linearized master equation in the weak-driving limit with $(g_{1,\mathrm{eff}}, g_{2,\mathrm{eff}}) = (5.0, 5.0)$ MHz [23]. All theoretical curve amplitudes have been scaled based on the peak empty cavity response.

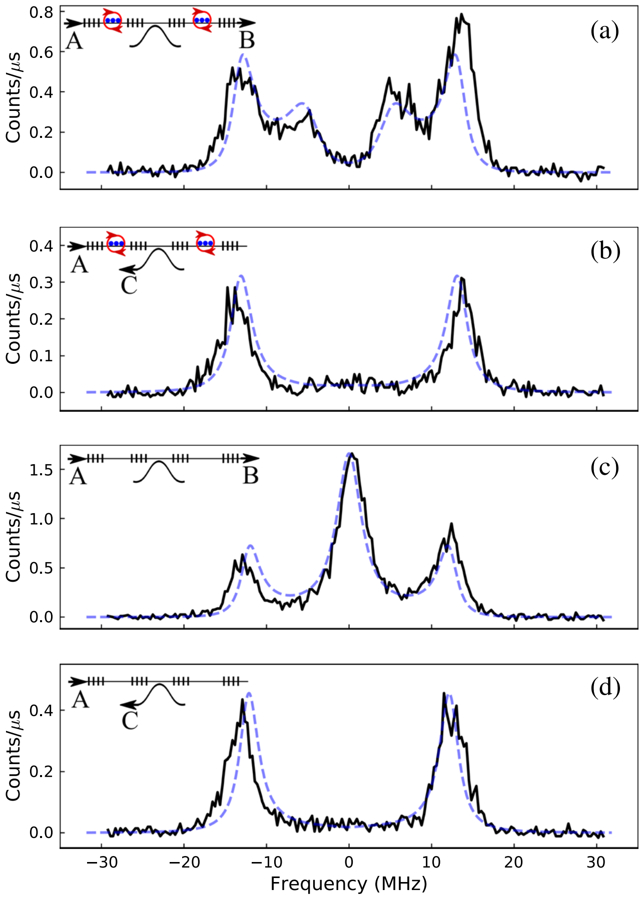

FIG. 2. Probing the fiber dark mode. (a)–(d) Data for the spectroscopy driving at port *A* for $(L_1, L_f, L_2) = (0.92, 1.40, 1.38)$ m and FBG reflectances (0.85,0.57,0.72,0.85). Data are overlaid with calculations performed with the single-mode linearized model [23]. The bare atomic and single-cavity resonances are located at 0 MHz. (a) Atoms are in both cavities and output is detected at port *B*. The fiber dark mode is visible as the doublet at ±5 MHz. The two symmetric bright modes are also observed at ±13.6 MHz. (b) Atoms are in both cavities and output is detected at port *C*. The fiber dark mode is absent, and only the two symmetric bright modes are observed. (c) Empty cavity spectra detected at port *B*. The central peak and the two sideband peaks correspond to the fiber dark mode and the two symmetric bright modes for coupled empty cavities. (d) Empty cavity spectra detected at port *C*. The fiber dark mode is absent. The probe drive strength at port *A* is 250 pW.

Next we show the results of driving and detecting the port *C* in Fig. 3. The central result of this experiment is the observation of the cavity dark mode at the atomic resonance (0 MHz) in Fig. 3(a). This mode is absent when driving the port *A* in Figs. 2(a) and 2(b), due to the direct excitation of cavity photons. Figure 3(b) indicates on-resonant suppression of the output at port *B*, confirming that the cavity dark mode does not support photonic excitations within the cavities. We note that the cavity dark mode signature is only observed in the case where both atomic ensembles are coupled to the cavities. In cases where atoms are coupled only to single cavities [Figs. 3(c) and 3(d)], the $C \rightarrow C$ resonant transmission is suppressed. In these singly loaded cases, we may interpret the experiment in two ways. First, we can consider the interaction of atoms with the on-resonant empty-cavity fiber dark mode [22]. This induces a vacuum Rabi splitting of the fiber dark mode, resulting in the observation of four unique spectroscopic peaks, and on-resonant suppression. Alternatively, one may view the system as the collective oscillation of four oscillators (three cavities and one atom), manifesting as two symmetric and two antisymmetric modes. In the case of four coupled oscillators, all oscillators are antinodes for all modes, resulting in their observation in Figs. 3(c) and 3(d). In

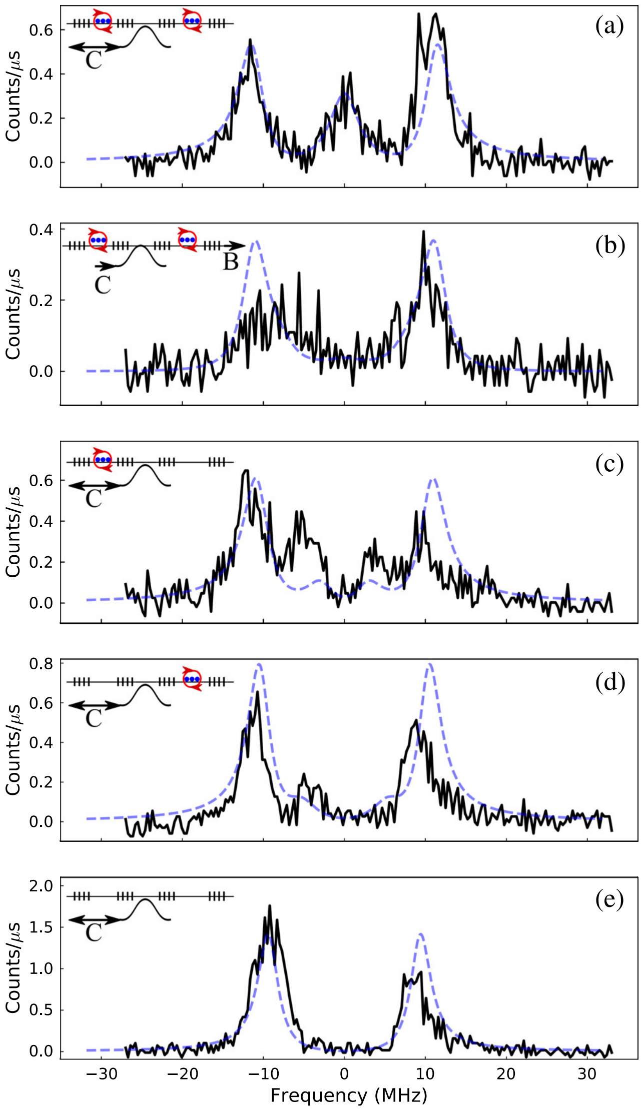

FIG. 3. Probing the cavity dark mode. (a)–(d) Data for the spectroscopy driving and detecting at port C for $(L_1, L_f, L_2) = (0.92, 1.80, 1.38)$ m and FBG reflectances (0.80,0.65,0.80,0.85). Dashed lines show theoretical calculations performed with the single-mode linearized model [23]. (a) Atoms are in both cavities ($C \to C$ spectroscopy). The cavity dark mode is visible as the central 0 MHz resonance. The two symmetric bright modes are also observed. (b) Atoms are in both cavities ($C \to B$ spectroscopy). Only the two bright modes are observed. (c) Atoms are in cavity 1 only ($C \to C$ spectroscopy). Four normal modes are observed. (d) Atoms are in cavity 2 only ($C \to C$ spectroscopy), and four normal modes are observed. (e) Empty cavity spectra ($C \to C$ spectroscopy), where two normal modes are observed. The input probe power at port C is 800 pW.

all cases, the data are in agreement with the theoretical curve with $(g_{1,\text{eff}}, g_{2,\text{eff}}) = (6.0, 7.0)$ MHz [23].

We note that the empty cavity responses in Figs. 2(c), 2(d), and 3(e) may be recovered in the model by setting $g = 0$, resulting in $|\text{FD1}\rangle$ and $|\text{FD2}\rangle$ coalescing to a single fiber dark mode, while $|\text{CD}\rangle$ vanishes.

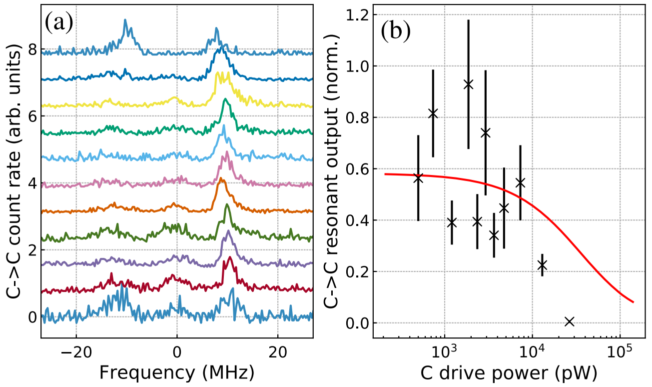

FIG. 4. Saturation of the dark mode. (a) $C \to C$ transmission curves for atoms loaded into both cavities, where increasing offset indicates increasing drive power (from 0.50 to 27 nW). (b) The on-resonant transmission is normalized with respect to the average amplitude of the two bright modes. The error bars are statistical. A theoretical curve is overlaid in red.

The above observation of the cavity dark mode for $C \to C$ transmission at zero detuning can be interpreted as *remote* excitation of atoms through the excitation of photons in the link fiber. Although no local photons are excited at the atom locations, we expect this dressed state to saturate at high drive powers. We expect the system response at high drive intensities to tend toward the empty-cavity dual peak spectrum of Fig. 3(e), and result in the dark mode signal diminishing with increasing intensity of excitation at the link fiber due to *remote* saturation of atoms.

Figure 4(a) confirms this hypothesis. The on-resonant peak is clearly resolved at low drive intensities, and is absent at high intensities. We therefore obtain the counterintuitive result that increasing drive strength *reduces* the on-resonant response of the link fiber cavity. We emphasize that the atoms do not experience *local* intensity on-resonance, because driving at C excites the cavity dark mode in the low intensity limit, and does not excite the fiber dark mode in the high intensity empty-cavity limit. The $C \to C$ saturation theoretical curve is obtained by solving the coupled semiclassical equations of motion describing the nonlinear dynamics [23], and agrees qualitatively with the cavity dark mode amplitudes plotted in Fig. 4(b). We attribute the enhanced saturation observed in the experiment to the asymmetric drive of the link fiber, which introduces a nonzero light level in cavity 2 for empty cavities. The saturation values used in the model are derived from a separate experiment driving from $A \to B$ for atoms in single cavities. From these data, we measure atom numbers of 370 and 250, saturation photon numbers of 40 and 20, and many-atom coupling strengths of 6.0 and 7.0 MHz in cavities 1 and 2, respectively.

We note that the asymmetry observed between the low- and high-frequency sides of the spectra in Figs. 2–4 when atoms are coupled to the cavities arises from the light shift of the off-resonant probe beam [23].

In conclusion, we have observed all five normal modes of a large coupled cavity QED system. In particular, we have observed the cavity dark mode, which is an excitation of atoms dressed with photons in a cavity which does not couple directly to either atomic ensemble. The nonlinear response of this mode shows remote excitation and saturation of atoms without photon excitations at the atom locations. We are especially interested in improving this system by overcoming technical challenges related to the simultaneous resonant locking of $N > 1$ optical cavities, and the trapping of single atoms in networked cavity QED systems.

The authors acknowledge the support of JST CREST Grant No. JPMJCR1771, JSPS KAKENHI Grants No. 16H01055 and No. 18H04293, and JST PRESTO Grant No. JPMJPR1662, Japan, and Institute for Advanced Theoretical and Experimental Physics, Waseda University. S. P. and N. N. thank the group of T. A. for the hospitality.

---

[*] takao@waseda.jp

[1] H. J. Kimble, Nature (London) **453**, 1023 (2008).
[2] A. Reiserer and G. Rempe, Rev. Mod. Phys. **87**, 1379 (2015).
[3] A. Serafini, S. Mancini, and S. Bose, Phys. Rev. Lett. **96**, 010503 (2006).
[4] J. I. Cirac, P. Zoller, H. J. Kimble, and H. Mabuchi, Phys. Rev. Lett. **78**, 3221 (1997).
[5] S. Ritter, C. Nölleke, C. Hahn, A. Reiserer, A. Neuzner, M. Uphoff, M. Mücke, E. Figueroa, J. Bochmann, and G. Rempe, Nature (London) **484**, 195 (2012).
[6] Y. Cao, G. C. Wang, H. D. Liu, and C. F. Sun, Sci. Rep. **8**, 5813 (2018).
[7] P. Törmä, Phys. Rev. Lett. **81**, 2185 (1998).
[8] M. J. Hartmann, F. G. S. L. Brandão, and M. B. Plenio, Nat. Phys. **2**, 849 (2006).
[9] A. D. Greentree, C. Tahan, J. H. Cole, and L. C. L. Hollenberg, Nat. Phys. **2**, 856 (2006).
[10] F. Le Kien and K. Hakuta, Phys. Rev. A **80**, 053826 (2009).
[11] C. Wuttke, M. Becker, S. Brückner, M. Rothhardt, and A. Rauschenbeutel, Opt. Lett. **37**, 1949 (2012).
[12] R. Yalla, M. Sadgrove, K. P. Nayak, and K. Hakuta, Phys. Rev. Lett. **113**, 143601 (2014).
[13] S. Kato and T. Aoki, Phys. Rev. Lett. **115**, 093603 (2015).
[14] W. Li, J. Du, V. G. Truong, and S. N. Chormaic, Appl. Phys. Lett. **110**, 253102 (2017).
[15] J. Keloth, K. P. Nayak, and K. Hakuta, Opt. Lett. **42**, 1003 (2017).
[16] D. E. Jones, G. T. Hickman, J. D. Franson, and T. B. Pittman, Opt. Lett. **41**, 3683 (2016).
[17] S. K. Ruddell, K. E. Webb, I. Herrera, A. S. Parkins, and M. D. Hoogerland, Optica **4**, 576 (2017).
[18] P. Schneeweiss, S. Zeiger, T. Hoinkes, A. Rauschenbeutel, and J. Volz, Opt. Lett. **42**, 85 (2017).
[19] M. D. Lukin, Rev. Mod. Phys. **75**, 457 (2003).
[20] K.-J. Boller, A. Imamoğlu, and S. E. Harris, Phys. Rev. Lett. **66**, 2593 (1991).
[21] C. Dong, V. Fiore, M. C. Kuzyk, and H. Wang, Science **338**, 1609 (2012).
[22] S. Kato, N. Német, K. Senga, S. Mizukami, X. Huang, S. Parkins, and T. Aoki, Nat. Commun. **10**, 1160 (2019).
[23] See Supplemental Material at http://link.aps.org/supplemental/10.1103/PhysRevLett.122.253603 for additional information on the theoretical modeling, experimental details, and a note on the asymmetry observed in the cavity spectra.
[24] F. Le Kien, V. I. Balykin, and K. Hakuta, J. Phys. Soc. Jpn. **74**, 910 (2005).
[25] E. Vetsch, D. Reitz, G. Sagué, R. Schmidt, S. T. Dawkins, and A. Rauschenbeutel, Phys. Rev. Lett. **104**, 203603 (2010).
[26] C. Lacroûte, K. S. Choi, A. Goban, D. J. Alton, D. Ding, N. P. Stern, and H. J. Kimble, New J. Phys. **14**, 023056 (2012).
[27] A. Goban, K. S. Choi, D. J. Alton, D. Ding, C. Lacroûte, M. Pototschnig, T. Thiele, N. P. Stern, and H. J. Kimble, Phys. Rev. Lett. **109**, 033603 (2012).